

The telegraph approximation for focused cosmic-ray transport in the presence of boundaries

Yuri E. Litvinenko, Frederic Effenberger¹

Department of Mathematics, University of Waikato, P. B. 3105, Hamilton, New Zealand

and

Reinhard Schlickeiser

*Institut für Theoretische Physik, Lehrstuhl IV: Weltraum- und Astrophysik,
Ruhr-Universität Bochum, D-44780 Bochum, Germany*

ABSTRACT

Diffusive cosmic-ray transport in nonuniform large-scale magnetic fields in the presence of boundaries is considered. Reflecting and absorbing boundary conditions are derived for a modified telegraph equation with a convective term. Analytical and numerical solutions of illustrative boundary problems are presented. The applicability and accuracy of the telegraph approximation for focused cosmic-ray transport in the presence of boundaries are discussed, and potential applications to modeling cosmic-ray transport are noted.

Subject headings: cosmic rays — diffusion — magnetic fields — scattering — Sun: particle emission

1. Introduction

When energetic cosmic-ray particles propagate in the cosmos, they often interact with turbulent magnetic fields. The evolution of a particle distribution is governed by the Fokker–Planck equation (e.g., Schlickeiser 2011, and references therein). When pitch-angle scattering is strong enough to ensure that the scale of density variation is significantly greater than the particle mean free path, the evolution can be approximated as a simpler diffusive process (Hasselmann & Wibberenz 1970; Schlickeiser & Shalchi 2008).

¹Present address: Department of Physics and KIPAC, Stanford University, Stanford 94305, USA

The diffusion approximation has been employed for studying the acceleration and propagation of energetic particles in various astrophysical situations—from the atmosphere of the Sun and interplanetary space (e.g., Bieber et al. 1987; Le Roux & Webb 2009; Artmann et al. 2011) to the interstellar medium (e.g., Schlickeiser, 2009; Litvinenko & Schlickeiser 2011; Schlickeiser et al. 2011). Observations reveal large-scale spatial variations of the magnetic field in all those locations (e.g., Sofue et al. 1986; Sandroos & Vainio 2007; Dröge et al. 2010). The diffusion model has been developed to incorporate the coherent particle streaming due to the effect of adiabatic focusing in a nonuniform background magnetic field (Earl 1981; Beeck & Wibberenz 1986; see also Litvinenko 2012a, 2012b; He & Schlickeiser 2014, and references therein).

Propagation of solar energetic particles in interplanetary magnetic fields remains a subject of intense research activity (e.g., Zhang et al. 2009; Dröge et al. 2010; Qin et al. 2013; Laitinen et al. 2013; Wang & Qin 2015). The theoretical studies are motivated by the new data from multi-point spacecraft observations, which allow new insights into the physics of the particle transport (e.g., Dresing et al. 2014; Dröge et al. 2014; Lario et al. 2014). Since theoretical modeling is usually based on numerical solutions, simple analytical approximations can complement and guide the simulations.

A general shortcoming of the diffusion approximation is that the diffusion equation implies an infinite speed of signal propagation, whereas particle speeds are finite, of course. A more accurate description may be provided by the telegraph equation (Goldstein 1951). This is an equation of hyperbolic type, and its solution at long times asymptotically approaches the solution of the diffusion equation (Davies 1954). The telegraph equation for Brownian motion (Brinkman 1956; Sack 1956) had been shown to be substantially more accurate than the diffusion equation (Hemmer 1961). The derivation of a generalized telegraph equation and its applications for modeling cosmic-ray transport had been repeatedly considered both in the limit of a uniform background magnetic field (e.g., Fisk & Axford 1969; Earl 1974, 1992; Gombosi et al. 1993; Schwadron & Gombosi 1994) and in the more realistic case of a spatially varying field (e.g., Earl 1976; Pauls & Burger 1994; Litvinenko & Noble 2013; Litvinenko & Schlickeiser 2013; Malkov & Sagdeev 2015).

Boundaries typically need to be considered in cosmic-ray transport problems in both interplanetary and interstellar plasmas (e.g., Schlickeiser 2009; Artmann et al. 2011). The boundary conditions for both the diffusion equation and the standard telegraph equation are well known (Masoliver et al. 1992, 1993). We are not aware of a published derivation of the corresponding boundary conditions for focused particle transport, described by a modified telegraph equation. In this paper, we develop the telegraph approximation for focused cosmic-ray transport in the presence of boundaries. The new analytical and numerical results

complement those for cosmic-ray transport in the absence of boundaries, which we presented in our previous study of the telegraph approximation (Effenberger & Litvinenko 2014).

Following a brief description of the model (Section 2), we derive the reflecting and absorbing boundary conditions (Section 3), illustrate the use of the Laplace transform and Fourier series for obtaining analytical solutions (Section 4), and compare them with numerical solutions of the Fokker–Planck equation (Section 5).

2. The telegraph approximation for focused cosmic-ray transport

Spatial non-uniformity of the mean magnetic field leads to the adiabatic focusing that results in coherent streaming of cosmic-ray particles along the mean field (Roelof 1969; Kunstmann 1979). Earl (1976) derived a modified telegraph equation for the focused particle transport in a spatially varying magnetic field. The equation, however, described the coefficient of an eigenfunction expansion rather than the particle density that is the physical quantity of interest. The problem was recently reexamined, and the telegraph approximation was derived for the particle density in a spatially varying magnetic field in a weak focusing limit (Litvinenko & Schlickeiser 2013). The telegraph approximation has also been obtained in a complementary case of an arbitrary constant focusing strength and isotropic pitch-angle scattering (Litvinenko & Noble 2013), using an exact expression for the variance of a particle distribution, obtained by Shalchi (2011).

A possible physical context for the telegraph approximation is provided by the Fokker–Planck equation for focused transport, which describes the evolution of the distribution function of energetic particles:

$$\frac{\partial f_0}{\partial t} + \mu v \frac{\partial f_0}{\partial z} + \frac{v}{2L}(1 - \mu^2) \frac{\partial f_0}{\partial \mu} = \frac{\partial}{\partial \mu} \left(D_{\mu\mu} \frac{\partial f_0}{\partial \mu} \right) \quad (1)$$

(Roelof 1969; Earl 1981). Here $f_0(z, \mu, v, t)$ is the distribution function (gyrotropic phase-space density), t is time, μ is the cosine of the particle pitch angle, v is the particle speed, z is the distance along the mean magnetic field B_0 , $L = -B_0/(\partial B_0/\partial z)$ is the adiabatic focusing length, and $D_{\mu\mu}$ is the Fokker–Planck coefficient for pitch-angle scattering.

To illustrate the application of the approximation to a model transport problem, we consider the simplest physically plausible model. Specifically, we assume a constant focusing length L , and we neglect momentum diffusion, adiabatic cooling, and advection with a background flow (say, the solar wind). The simplifying assumptions are discussed, for example, by Artmann et al. (2011) and Effenberger & Litvinenko (2014) in the context of solar energetic particle transport in interplanetary space.

The distribution function can be expressed as the sum of the isotropic density F_0 and an anisotropic component g_0 :

$$f_0(z, \mu, t) = F_0(z, t) + g_0(z, \mu, t), \quad (2)$$

where

$$F_0(z, t) = \frac{1}{2} \int_{-1}^1 f_0 d\mu. \quad (3)$$

Assuming that $g_0 \ll F_0$, an approximate expression for g_0 can be found and substituted into Equation (1), integrated with respect to μ . Depending on the accuracy of the expression for g_0 , the result is either the usual diffusion approximation or the telegraph approximation for focused transport (e.g., Earl 1976; Litvinenko & Schlickeiser 2013). Here we investigate the modified telegraph equation for the isotropic density:

$$\frac{\partial F_0}{\partial t} + \tau \frac{\partial^2 F_0}{\partial t^2} = \kappa_{\parallel} \frac{\partial^2 F_0}{\partial z^2} + \xi \kappa_{\parallel} \frac{\partial F_0}{\partial z}, \quad (4)$$

where $\xi \kappa_{\parallel}$ is the coherent speed (e.g., Earl 1981), κ_{\parallel} is the parallel diffusion coefficient, $\xi = \lambda_0/L$ is the focusing strength, and λ_0 is the scattering mean free path in the absence of focusing ($\xi = 0$). Equation (4) is written in dimensionless form by measuring distances in units of λ_0 , speed in units of the constant particle speed v , and time in units of λ_0/v . Although we formally recover the diffusion approximation by setting $\tau = 0$, in practice τ is of order unity in a physically relevant parameter range (Litvinenko & Schlickeiser 2013).

The coefficients κ_{\parallel} and τ generally depend on the focusing strength ξ . In the weak focusing limit $\xi^2 \ll 1$, the transport coefficients are given by Equations (9) and (14) in Litvinenko & Schlickeiser (2013) for an arbitrary pitch-angle scattering coefficient $D_{\mu\mu}$. For isotropic scattering, the telegraph equation has been derived for an arbitrary focusing strength ξ , and κ_{\parallel} and τ are given by Equations (9) and (24) in Litvinenko & Noble (2013). The complementary expressions agree in the limit of weak focusing and isotropic scattering.

It is worth noting that the derivation of the telegraph equation by Earl (1973) and Litvinenko & Schlickeiser (2013) involves truncating an infinite system, equivalent to the original Fokker–Planck equation. A well-known weakness of that approach (Gombosi et al. 1993; Schwadron & Gombosi 1994) has been recently reiterated by Malkov & Sagdeev (2015). Truncating the system of harmonics, derived from the Fokker–Planck equation, leads to an error in the coefficient τ —and more generally, to an equation which is not correctly ordered. The correct way of deriving the telegraph equation relies on an asymptotic expansion that yields the diffusion equation in the lowest order and the telegraph equation in the next order. Gombosi et al. (1993) described the method in detail for the case of a uniform background magnetic field and isotropic scattering. Of course the correct mathematical procedure is generally preferable. In practice, however, the improvement in accuracy may be quite modest.

For instance, Gombosi et al. used the parameter τ to calculate the signal propagation speed in the telegraph equation by both methods. The correct derivation gave $v\sqrt{5/11}$, where v is the particle speed, compared with $v\sqrt{1/3}$ when simple truncation was used—about 17% difference. Effenberger and Litvinenko (2014) showed that the telegraph equation for focused transport, obtained by the simpler method, yields a solution that agrees well with the numerical solution of the original Fokker–Planck equation on an infinite interval. It is also worth stressing that the telegraph approximation was shown to reproduce the evolution of the particle density profile much more accurately than the diffusion approximation ($\tau = 0$), especially when the focusing is strong (Litvinenko & Noble 2013; Effenberger & Litvinenko 2014).

It may be useful to rewrite Equation (1) in terms of the linear density

$$F(z, t) = \exp(\xi z) F_0(z, t), \quad (5)$$

which is the number of particles per line of force per unit distance parallel to the mean magnetic field. Clearly, the linear density satisfies

$$\frac{\partial F}{\partial t} + \tau \frac{\partial^2 F}{\partial t^2} = \kappa_{\parallel} \frac{\partial^2 F}{\partial z^2} - \xi \kappa_{\parallel} \frac{\partial F}{\partial z}. \quad (6)$$

The descriptions in terms of F_0 and F are mathematically equivalent, and the choice of F_0 or F is a matter of convenience (Earl 1981). For instance, particle conservation in the absence of sources and sinks is conveniently expressed as

$$N(t) = 2 \int F dz = \text{const.} \quad (7)$$

Note for clarity that Litvinenko & Schlickeiser (2013) did not work with the linear density and they used the notation $F(z, t)$ instead of $F_0(z, t)$.

3. Boundary conditions

Masoliver et al. (1992, 1993) obtained boundary conditions for the standard telegraph equation in the presence of reflecting or absorbing boundaries. We generalize the arguments in Masoliver et al. (1992, 1993) and derive the boundary conditions for a modified telegraph equation with a convective term that can describe the focused cosmic-ray transport.

Decomposing the particle distribution function into two components corresponding to particles moving to the right, $a(z, t)$, and to the left, $b(z, t)$, we have the coupled equations that reduce to Equation (1) in Masoliver et al. (1992) in the limit $\xi = 0$:

$$\partial_t a = -\sqrt{\frac{\kappa_{\parallel}}{\tau}} \partial_z a + \frac{1}{2\tau} (b - a) + \frac{1}{2} \xi \sqrt{\frac{\kappa_{\parallel}}{\tau}} (a + b), \quad (8)$$

$$\partial_t b = \sqrt{\frac{\kappa_{\parallel}}{\tau}} \partial_z b + \frac{1}{2\tau} (a - b) - \frac{1}{2} \xi \sqrt{\frac{\kappa_{\parallel}}{\tau}} (a + b). \quad (9)$$

The linear density

$$F(z, t) = a + b \quad (10)$$

satisfies the focused telegraph equation (6). Physically, $w = \sqrt{\kappa_{\parallel}/\tau}$ is a signal propagation speed in the telegraph equation, which does not depend on the first-order terms in the equation. The first term on the right in Equation (8) describes convective transport, the second term describes the particle change of direction, and the third term describes the focusing effect of a nonuniform background magnetic field. The interpretation is similar for Equation (9).

Consider first a region $z_1 \leq z \leq z_2$ with absorbing boundaries at $z = z_1$ and $z = z_2$, so that

$$a(z_1, t) = 0, \quad b(z_2, t) = 0. \quad (11)$$

Subtracting Equation (9) from Equation (8) and using Equation (11) yields the boundary conditions

$$\pm \sqrt{\kappa_{\parallel}\tau} (\partial_z F - \xi F) = F + \tau \partial_t F, \quad (12)$$

where the plus (minus) sign corresponds to the left (right) boundary at $z = z_1$ ($z = z_2$). The absorbing boundary conditions for the density F_0 follow from Equations (5) and (12):

$$\pm \sqrt{\kappa_{\parallel}\tau} \partial_z F_0 = F_0 + \tau \partial_t F_0. \quad (13)$$

If we formally set $\tau = 0$, the telegraph approximation simplifies to the focused diffusion model, termed pseudo-diffusion by Earl (1981), and the absorbing boundary conditions above simplify to the familiar condition $F_0 = F = 0$ at an absorbing boundary.

Now suppose that reflecting boundaries are present at $z = z_1$ and $z = z_2$, so that

$$a(z_1, t) = b(z_1, t), \quad a(z_2, t) = b(z_2, t). \quad (14)$$

In this case, subtracting Equation (9) from Equation (8) and using Equation (14) leads to the boundary conditions

$$\partial_z F - \xi F = 0 \quad (15)$$

and

$$\partial_z F_0 = 0 \quad (16)$$

at $z = z_1$ and $z = z_2$, which are the same conditions as those for both the diffusion equation and the telegraph equation considered by Masoliver et al. (1993). In the case of a single reflecting boundary, Equation (15) immediately follows on integrating Equation (6) and using the particle conservation given by Equation (7).

Finally, we note that Marshak (1947) advocated the use of an escape condition for the particle flux

$$S = \frac{v}{2} \int_{-1}^1 \mu g_0 d\mu \quad (17)$$

as a more accurate alternative to the conventional absorbing boundary condition. Marshak's condition is given by

$$S = \int_{-1}^0 \mu v F_0 d\mu \quad (18)$$

at the left boundary and

$$S = \int_0^1 \mu v F_0 d\mu \quad (19)$$

at the right boundary. For example, in the weak focusing limit of the telegraph approximation, the flux is given by Equation (13) in Litvinenko & Schlickeiser (2013), which yields

$$-\kappa_{\parallel} \partial_z F_0 + \tau \kappa_{\parallel} \partial_{tz} F_0 = \pm \frac{1}{2} F_0 \quad (20)$$

in our dimensionless units, where the minus (plus) sign corresponds to the left (right) boundary at $z = z_1$ ($z = z_2$). In the limit $\tau = 0$, the condition reduces to the corresponding boundary condition of the diffusion model (Weinberg & Wigner 1958). In practice, the presence of a second mixed derivative $\partial_{tz} F_0$ in Equation (20) makes the boundary condition difficult to use.

4. Analytical solutions

4.1. Infinite interval

Analytical solutions of the focused diffusion model are commonly used to model the transport of solar energetic particles in interplanetary space (e.g., Artmann et al. 2011 and references therein). Since the telegraph approximation should give a more accurate description of the cosmic-ray transport, analytical solutions of the telegraph approximation could be used to quantify the accuracy of the diffusion approximation or to validate the accuracy of a numerical solution of the Fokker–Planck equation for an evolving particle distribution function. Here we illustrate how initial and boundary value problems for the modified telegraph equation can be solved by Laplace transform for infinite and semi-infinite intervals and by Fourier series for a finite interval.

For simplicity we assume a symmetric point source at $z = z_0$, so that $a(z, 0) = b(z, 0)$, and the initial conditions are given by

$$F_0(z, 0) = \delta(z - z_0), \quad \partial_t F_0(z, 0) = 0, \quad (21)$$

where the second condition follows from Equations (8) and (9). The telegraph equation is linear, and so we omit the normalization constant $\frac{1}{2} \exp(-\xi z_0)N$ in $F_0(z, 0)$ for brevity.

Consider first the initial value problem for an infinite interval. Although in this case the solution can be obtained by a change of variables, which reduces Equation (4) to the standard telegraph equation (e.g., Kevorkian 2000), it is instructive to solve the problem directly using the Laplace transform. The transform of Equation (4) reads

$$\tilde{F}_0'' + \xi \tilde{F}_0' - \frac{1}{\kappa_{\parallel}} s(1 + \tau s) \tilde{F}_0 = -\frac{1}{\kappa_{\parallel}} (1 + \tau s) \delta(z - z_0), \quad (22)$$

with the Laplace transform $\tilde{F}_0(z, s) = L[F_0(z, t)]$ and the prime denotes differentiation with respect to z . Solving the ordinary differential equation yields the transform

$$\tilde{F}_0(z, s) = \frac{1 + \tau s}{2\kappa_{\parallel}\eta} \exp\left(-\frac{\xi}{2}(z - z_0) - \eta|z - z_0|\right), \quad (23)$$

where

$$\eta = \sqrt{\frac{\xi^2}{4} + \frac{s(1 + \tau s)}{\kappa_{\parallel}}}. \quad (24)$$

Consequently the solution of the initial value problem is given by

$$F_0(z, t) = G_0 + \tau \partial_t G_0, \quad (25)$$

where

$$G_0(z, t) = L^{-1} \left[\frac{1}{2\kappa_{\parallel}\eta} \exp\left(-\frac{\xi}{2}(z - z_0) - \eta|z - z_0|\right) \right] \quad (26)$$

is the fundamental solution of the modified telegraph equation. Evaluating the inverse transform yields

$$G_0(z, t) = \frac{1}{2\sqrt{\kappa_{\parallel}\tau}} \exp\left(-\frac{\xi}{2}(z - z_0) - \frac{t}{2\tau}\right) I_0(u) H\left(t - \sqrt{\frac{\tau}{\kappa_{\parallel}}}|z - z_0|\right). \quad (27)$$

Here, H is the Heaviside step function, I_0 is a modified Bessel function, and its argument is

$$u = \frac{1}{2} \sqrt{(1 - \xi^2 \kappa_{\parallel} \tau) \left(\frac{t^2}{\tau^2} - \frac{(z - z_0)^2}{\kappa_{\parallel} \tau} \right)}. \quad (28)$$

Note that we assume $\xi^2 \kappa_{\parallel} \tau < 1$. The inequality was shown to be valid both in the case of weak focusing and anisotropic scattering (Litvinenko & Schlickeiser 2013) and in the case of strong focusing and isotropic scattering (Litvinenko & Noble 2013). For instance,

$(1 - \xi^2 \kappa_{\parallel} \tau) / \tau = 1$ for isotropic scattering. Substituting Equation (27) into Equation (25) leads to a solution in terms of the modified Bessel functions I_0 and I_1 :

$$F_0(z, t) = \frac{1}{4\sqrt{\kappa_{\parallel}\tau}} \exp\left(-\frac{\xi}{2}(z - z_0) - \frac{t}{2\tau}\right) \times \\ \left[I_0(u) + (1 - \xi^2 \kappa_{\parallel} \tau) \frac{t}{2\tau} \frac{I_1(u)}{u} \right] H\left(t - \sqrt{\frac{\tau}{\kappa_{\parallel}}} |z - z_0|\right) \\ + \frac{1}{2} \exp\left(-\frac{\xi}{2}(z - z_0) - \frac{t}{2\tau}\right) \left[\delta\left(\sqrt{\frac{\kappa_{\parallel}}{\tau}} t - (z - z_0)\right) + \delta\left(\sqrt{\frac{\kappa_{\parallel}}{\tau}} t + (z - z_0)\right) \right], \quad (29)$$

which slightly generalizes Equations (18) and (19) in Effenberger & Litvinenko (2014) who compared the solution with both the prediction of the diffusion model and a numerical solution of the original Fokker–Planck equation.

4.2. Semi-infinite interval: a reflecting boundary

Now consider the initial value problem, specified by Equations (16) and (21), on a semi-infinite interval $z > 0$. Physically, a reflecting inner boundary condition at $z_1 = 0$ may correspond to the transport of solar energetic particles, accelerated close to the solar surface. The reflection of particles traveling towards the sun is caused by a magnetic bottle effect of the strongly converging magnetic field. In this case the solution of the transformed Equation (22), which satisfies $\partial_z \tilde{F}_0(0, s) = 0$, is given by

$$\tilde{F}_0(z, s) = \frac{1 + \tau s}{\kappa_{\parallel} \eta (2\eta + \xi)} \exp\left(-\frac{\xi}{2}(z - z_0)\right) \times \\ \left[\left(\eta + \frac{1}{2}\xi\right) \exp(-\eta|z - z_0|) + \left(\eta - \frac{1}{2}\xi\right) \exp(-\eta(z + z_0)) \right]. \quad (30)$$

As an interesting aside, note that the mean age T of particles at a given location z can be elegantly expressed in terms of the Laplace transform \tilde{F}_0 :

$$T = \frac{\int_0^\infty t F_0 dt}{\int_0^\infty F_0 dt} = -\partial_s \tilde{F}_0(z, 0). \quad (31)$$

For example, suppose that a particle source is located very close to the solar surface, so that we may take $z_0 = 0$. We calculate

$$T = \frac{1}{\kappa_{\parallel} \xi^2} + \frac{z}{\kappa_{\parallel} \xi} - \tau, \quad (32)$$

which agrees with the advection-dominated limit of Equation (4) in Jokipii (1976).

The solution of the initial value problem is again given by Equation (25), but now the fundamental solution is as follows:

$$G_0(z, t) = L^{-1} \left[\frac{1}{2\kappa_{\parallel}\eta} \exp \left(-\frac{\xi}{2}(z - z_0) \right) \left[\exp(-\eta|z - z_0|) + \frac{2\eta - \xi}{2\eta + \xi} \exp(-\eta(z + z_0)) \right] \right]. \quad (33)$$

For simplicity, consider again a particle source located near the boundary. Setting $z_0 = 0$ and keeping in mind that $z > 0$, we have

$$G_0(z, t) = L^{-1} \left[\frac{2}{\kappa_{\parallel}(2\eta + \xi)} \exp \left(-\frac{1}{2}(2\eta + \xi)z \right) \right]. \quad (34)$$

The inverse Laplace transform can be expressed in terms of a table transform (Erdélyi et al. 1954) by noticing that

$$\eta^2 = \frac{\tau}{\kappa_{\parallel}} \left[\left(s + \frac{1}{2\tau} \right)^2 - \alpha^2 \right] \quad (35)$$

where

$$\alpha^2 = \frac{1 - \xi^2 \kappa_{\parallel} \tau}{4\tau^2}. \quad (36)$$

The resulting fundamental solution is as follows:

$$G_0(z, t) = \frac{1}{\sqrt{\kappa_{\parallel}\tau}} \exp \left(-\frac{t}{2\tau} \right) H \left(t - \sqrt{\frac{\tau}{\kappa_{\parallel}}} z \right) \times \left[\exp \left(-\frac{\xi}{2} \sqrt{\frac{\kappa_{\parallel}}{\tau}} t \right) + \alpha \int_0^{\sqrt{t^2 - \tau z^2 / \kappa_{\parallel}}} \exp \left(-\frac{\xi}{2} \sqrt{\frac{\kappa_{\parallel}}{\tau}} \sqrt{t^2 - w^2} \right) I_1(\alpha w) dw \right]. \quad (37)$$

The result can be verified in the limiting case of a uniform magnetic field ($\xi = 0$) when the solution simplifies to

$$G_0(z, t) = \frac{1}{\sqrt{\kappa_{\parallel}\tau}} \exp \left(-\frac{t}{2\tau} \right) I_0(u_0) H \left(t - \sqrt{\frac{\tau}{\kappa_{\parallel}}} z \right) \quad (38)$$

where

$$u_0 = \frac{1}{2} \sqrt{\frac{t^2}{\tau^2} - \frac{z^2}{\kappa_{\parallel}\tau}}. \quad (39)$$

Consequently,

$$F_0(z, t) = \frac{1}{2\sqrt{\kappa_{\parallel}\tau}} \exp \left(-\frac{t}{2\tau} \right) \left[I_0(u_0) + \frac{t}{2\tau} \frac{I_1(u_0)}{u_0} \right] H \left(t - \sqrt{\frac{\tau}{\kappa_{\parallel}}} z \right) + \exp \left(-\frac{t}{2\tau} \right) \delta \left(\sqrt{\frac{\kappa_{\parallel}}{\tau}} t - z \right). \quad (40)$$

In other words, the solution on the semi-infinite interval $z > 0$ with a source at the edge of the interval in the absence of focusing is simply double the solution of the corresponding initial value problem for an infinite interval. The result immediately follows on applying the method of images to the problem.

Finally, for a uniform magnetic field, the solution on a semi-infinite interval with an absorbing boundary is given by Equation (19) in Masoliver et al. (1992).

4.3. Finite interval: reflecting boundaries

The relatively simple form of the reflecting boundary conditions makes it possible to express the solution of the telegraph equation on a finite interval in terms of a Fourier series. The series solution is particularly convenient for long times, when the first few terms of the series accurately approximate the solution. Suppose that two reflecting boundaries are present at $z_1 = 0$ and $z_2 = l$, $F_0(z, 0)$ is given for $0 < z < l$, and $\partial_t F_0(z, 0) = 0$ for simplicity. Straightforward application of the method of separation of variables to Equations (4) and (16) leads to

$$F_0(z, t) = c_0 + \sum_{n=1}^{\infty} c_n Z_n(z) T_n(t), \quad (41)$$

where

$$Z_n(z) = \exp\left(-\frac{\xi z}{2}\right) \left[\cos\left(\frac{\pi n z}{l}\right) + \frac{\xi l}{2\pi n} \sin\left(\frac{\pi n z}{l}\right) \right], \quad (42)$$

$$T_n(t) = \exp\left(-\frac{t}{2\tau}\right) \left[\cosh \omega_n t + \frac{1}{2\omega_n \tau} \sinh \omega_n t \right], \quad (43)$$

$$\omega_n = \left[\frac{1}{4\tau^2} - \frac{\kappa_{\parallel}}{\tau} \left(\frac{\xi^2}{4} + \left(\frac{\pi n}{l} \right)^2 \right) \right]^{1/2}. \quad (44)$$

The initial conditions yield

$$c_0 = \frac{\xi}{[\exp(\xi l) - 1]} \int_0^l \exp(\xi z) F_0(z, 0) dz, \quad (45)$$

$$c_n = \frac{2}{l} \left[1 + \left(\frac{\xi l}{2\pi n} \right)^2 \right]^{-1} \int_0^l \exp\left(\frac{\xi z}{2}\right) \left[\cos\left(\frac{\pi n z}{l}\right) + \frac{\xi l}{2\pi n} \sin\left(\frac{\pi n z}{l}\right) \right] F_0(z, 0) dz. \quad (46)$$

In the limit $\xi = 0$, the solution for the initial profile $F_0(z, 0) = \delta(z - z_0)$ agrees with Equation (19) in Masoliver et al. (1993).

4.4. Finite interval: absorbing boundaries

The appearance of two partial derivatives in Equation (13) complicates the solution of the telegraph equation with absorbing boundaries. In the case $\xi = 0$ and $F_0(z, 0) = \delta(z - z_0)$, Equation (25) in Masoliver et al. (1992) gives an exact solution in terms of an infinite series of Bessel functions. Since numerical solutions might not capture important qualitative features of the solution, it is natural to seek an approximate analytical solution. Here, we illustrate an integral approximation method, similar to the heat-balance approximation in heat conduction (e.g., Crank 1984; Hill & Dewynne 1987).

Consider a finite region with absorbing boundaries at $z_1 = 0$ and $z_2 = l$. The boundary value problem for Equation (4) might serve as the basis for a simple model for the escape of galactic cosmic rays away from the galactic plane (Schlickeiser 2009). The idea of the approximation is that, instead of solving Equation (4) exactly, we integrate it with respect to z from 0 to l and seek a solution of a specified functional form that satisfies the boundary conditions. As a simple illustration, consider

$$F_0(z, t) \approx f_1(z)f_2(t) \quad (47)$$

and require that it satisfies both the absorbing boundary conditions, given by Equation (13), and an ordinary differential equation for $f_2(t)$, obtained by integrating Equation (4) over z . On choosing a parabolic density profile

$$f_1(z) = 1 + kz(l - z), \quad (48)$$

it is straightforward to verify that

$$\tau \ddot{f}_2 + \dot{f}_2 + \frac{2\kappa_{\parallel}k}{1 + kl^2/6} f_2 = 0, \quad (49)$$

and so a possible solution is given by

$$f_2(t) = \text{const} \exp(\lambda t), \quad (50)$$

where the constants k and λ follow from Equation (49) and the boundary conditions:

$$k = \frac{1 + \lambda\tau}{\sqrt{\kappa_{\parallel}\tau}l}, \quad (51)$$

$$\lambda = -\frac{2}{l} \sqrt{\frac{\kappa_{\parallel}}{\tau}} \frac{1}{1 + kl^2/6}. \quad (52)$$

It follows that

$$\lambda = -\frac{1}{2\tau} - \frac{3}{l} \sqrt{\frac{\kappa_{\parallel}}{\tau}} \pm \sqrt{\left(\frac{1}{2\tau} + \frac{3}{l} \sqrt{\frac{\kappa_{\parallel}}{\tau}}\right)^2 - \frac{12\kappa_{\parallel}}{\tau l^2}}, \quad (53)$$

and so the approximate solution describes the evolution of an initially broad (parabolic) particle density profile.

5. Stochastic simulations of the Fokker–Planck equation

5.1. Numerical method

To quantitatively assess the accuracy of the telegraph approximation in the presence of boundaries, we use numerical solutions of the corresponding Fokker–Planck equation. The numerical approach is based on solutions to an equivalent system of stochastic differential equations (SDEs), similar to the method employed in Litvinenko & Noble (2013) and Effenberger & Litvinenko (2014). In the following, we use the Milstein approximation scheme, given by Equations (29) and (30) in Effenberger & Litvinenko (2014), and we refer the reader to this paper for more details on the numerics (see also Kopp et al. 2012, and references therein for more details on the SDE method).

In the present study, we have to take special care of the boundary conditions required for the Fokker–Planck equation. In practice, this means that the trajectories of pseudo-particles are integrated according to their stochastic evolution equations, until they cross a boundary (say at $z = 0$ or $z = l$). At this point, either the particle speed is reversed (and so its pitch angle changes its sign at a reflecting boundary) or the particle is discarded for the rest of the simulation at an absorbing boundary. The final distribution function is constructed in the usual way, by applying an appropriate binning procedure to the particle positions, and normalizing the result for comparison with the analytic predictions.

We consider the case of isotropic scattering, for which the Fokker–Planck pitch-angle scattering coefficient $D_{\mu\mu}$ is given by

$$D_{\mu\mu} = D_0(1 - \mu^2). \quad (54)$$

In this case, the coefficients in the telegraph equation (4) are given by

$$\kappa_{\parallel} = \frac{\coth \xi}{\xi} - \frac{1}{\xi^2}, \quad (55)$$

$$\tau = \frac{\tanh \xi}{\xi} \quad (56)$$

(Litvinenko & Noble 2013; He & Schlickeiser 2014, and references therein). We have $\kappa_{\parallel} \approx 1/3$ and $\tau \approx 1$ in the weak focusing limit $\xi^2 \ll 1$.

5.2. Semi-infinite interval: a reflecting boundary

We first consider the positive semi-infinite region with a reflecting boundary at $z = 0$. Particles are injected at time $t_0 = 0$ and position $z_0 = 1$ with isotropic pitch angle. Masoliver

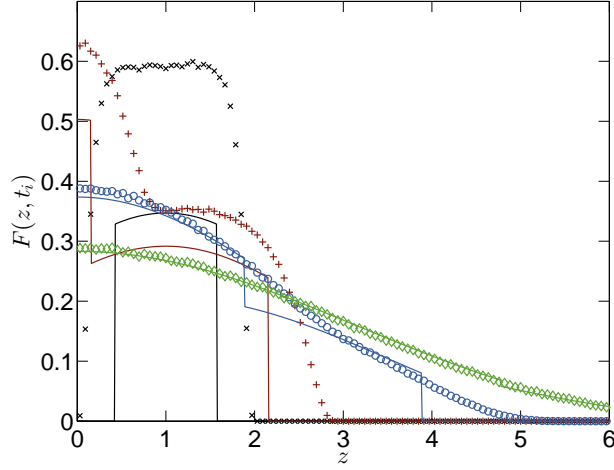


Fig. 1.— Isotropic density $F(z, t_i)$ at four different times $t_1 = 1$ (black, 'x'), $t_2 = 2$ (red, '+'), $t_3 = 5$ (blue, 'o') and $t_4 = 10$ (green, '◇') for the semi-infinite domain with reflecting boundary. The solid lines show the solution of the telegraph equation, given by Equation (57). The symbols show the numerical results, obtained from 10^6 particles starting at $z_0 = 1.0$, and averaging without regard to the pitch angle of the particles.

et al. (1993) gave a solution for the telegraph equation for a case without focusing based on the method of images (their Equations (14) and (16)). Their solution follows from our Equation (29) in the limit $\xi \rightarrow 0$ when we apply the method of images:

$$F^{\text{refl}}(z, t) = F_0(z, t|z_0) + F_0(z, t|-z_0), \quad (57)$$

where $F_0(z, t|z_0)$ denotes the solution with injection at z_0 . Note for clarity that in Masoliver et al. (1993) the signal propagation speed is denoted as c and their T is equal to our τ . The method of images is not applicable in the case $\xi \neq 0$.

We concentrate on the case $\xi = 0$ to describe the effect of the boundaries on the particle distribution. We compare the analytical solution for the semi-infinite domain with simulation results for the Fokker–Planck equation as described above. Figure 1 shows the evolution of the particle distribution at four different times, calculated from an injection of 10^6 pseudo-particles. The comparison shows a good agreement after a few scattering times, as was the case for the solution on an infinite interval (Effenberger & Litvinenko 2014). The disagreement between the numerical and approximate analytical solutions, however, is significant at earlier times. The overall amplitude of the distribution appears to be underestimated by the telegraph solution. Note that, while the telegraph solution conserves the particle number, the δ -functional contributions are omitted in Figure 1. Furthermore, the slower signal propagation speed, when compared to the particle speed, results in positions of

the discontinuities, which underestimate the fast particle spread beyond the limits imposed by the signal propagation speed, especially at early times. At times $t = 5$ and $t = 10$ the agreement is significantly better, and the discontinuities have almost disappeared.

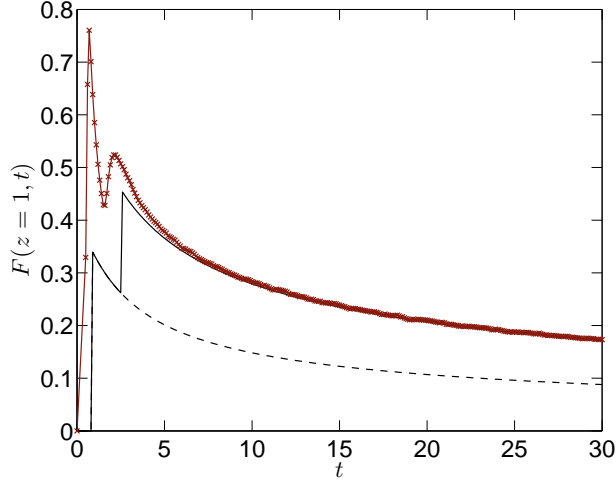


Fig. 2.— Time profile at $z = 1$ for the semi-infinite interval with a reflecting left boundary. Particles are injected at $z_0 = 0.5$ to illustrate the reflection effect and the resulting discontinuities in the telegraph solution. The solid black line gives the solution of Equation (57), while the dashed line gives the solution for an infinite interval (without a reflecting boundary at the origin). The symbols connected with a red line show the numerical SDE solution obtained from the injection of 10^6 particles.

In addition to the spatial density profiles, time profiles of particle intensities can provide an important tool for analyzing solar energetic particle data. Figure 2 illustrates the effect of a reflecting boundary at $z = 0$, say due to the magnetic mirroring of energetic particles accelerated in the solar corona. To emphasize the effect of the reflecting boundary for illustrative purposes, we assume that the particle injection occurs at $z_0 = 0.5$ and plot the time profile at $z = 1$. A jump in the particle intensity caused by the arrival of reflected particles is clearly visible. The early arrival of non-scattered particles at dimensionless time $t = (z - z_0)/v = 0.5$ causes the discrepancy between the numerical Fokker–Planck solution and the telegraph approximation, which almost disappears when the diffusing reflected particles start arriving at time $t = (z + z_0)/w \approx 2.6$ and decreases even further as the transport becomes more diffusive for later times.

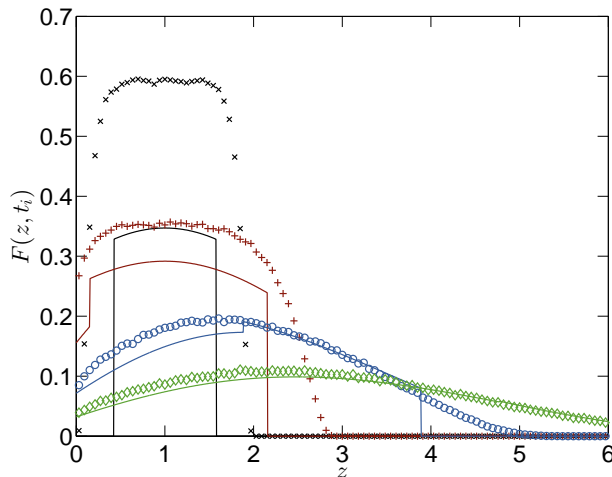


Fig. 3.— Similar to Figure 1, but now with an absorbing left boundary condition.

5.3. Semi-infinite interval: an absorbing boundary

We consider a setting similar to the one in Section 5.2, with initial particle injection again at $z_0 = 1$, but now for a left-hand side absorbing boundary condition on the semi-infinite interval. Figure 3 compares the analytic result for the case without focusing (Equation (19) in Masoliver et al. 1992) with the numerical Fokker–Planck results for 10^6 particles. For the purpose of comparison, the solution of Masoliver needs to be rescaled with $z = cy$ and normalized with the signal speed, due to the different nondimensionalization.

As in the previous case with reflecting boundary conditions, we find that the agreement of the analytical and numerical solutions improves as later times. A noteworthy feature is the non-vanishing boundary values at an absorbing boundary, in contrast to the boundary condition $F = F_0 = 0$ in the diffusion approximation (see also Section 5.5 below).

5.4. Finite interval: reflecting boundaries

As the next example, we consider a finite interval with reflecting boundaries. We evaluate equation (41) with $N = 1000$ terms in the Fourier series on a finite domain of length $l = 10$ with an isotropic injection of particles at $z_0 = 2.5$. Figure 4 shows a comparison between this result and a stochastic simulation of 10^6 particles giving a solution to the corresponding Fokker–Planck Equation (1). We consider the cases of no focusing ($\xi = 0$) and strong focusing ($\xi = 1.5$).

At relatively early times, say $t_1 = 5$, the Fourier series solution shows limited applicabil-

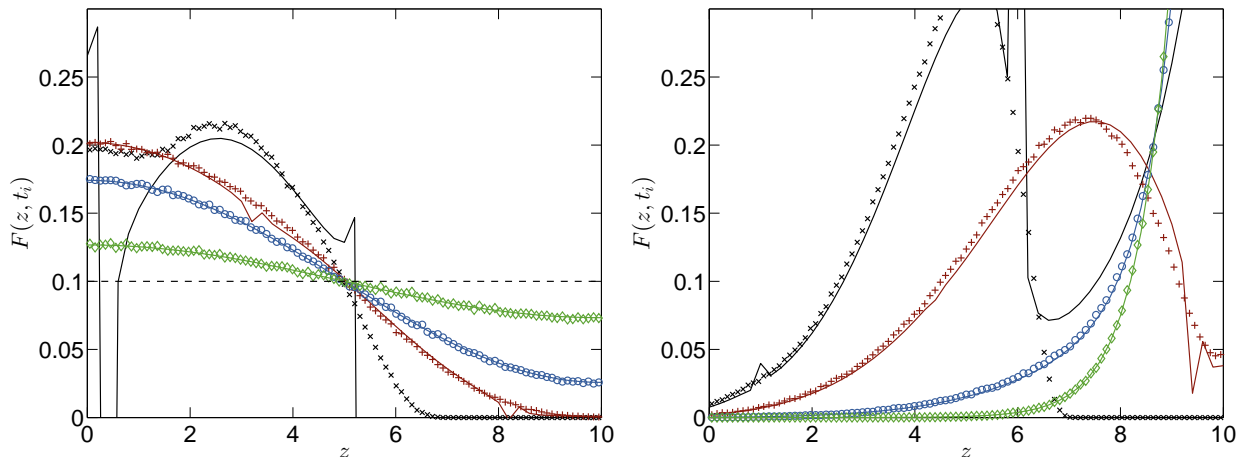


Fig. 4.— No focusing ($\xi = 0$, left panel) and strong focusing ($\xi = 1.5$, right panel) results for the isotropic linear density $F(z, t_i)$ on a finite domain of length $l = 10$ with injection at $z_0 = 2.5$ and reflecting boundaries. The four different times displayed are $t_1 = 5$ (black, 'x'), $t_2 = 10$ (red, '+'), $t_3 = 20$ (blue, 'o') and $t_4 = 50$ (green, '◇'). The solid lines show the solution of the telegraph equation, given by Equation (41). The symbols show the numerical results, obtained from 10^6 particles starting at z_0 . In the left panel, the dashed line indicates the constant steady-state solution.

ity near the discontinuities in the solution of the telegraph equation. Similar to the previous cases of infinite and semi-infinite domain, the Fokker–Planck solution exhibits a relatively smooth profile at the discontinuities, and at later stages the agreement is very good, both for weak and strong focusing. For long times, the solution approaches the steady state solution, given by the term c_0 in Equation (41):

$$F_0(z, t \rightarrow \infty) \rightarrow c_0 = \frac{\xi N}{2(\exp(\xi l) - 1)}, \quad (58)$$

which reduces to $F_0 = N/2l$ in the limit $\xi = 0$.

5.5. Finite interval: absorbing boundaries

Finally, we consider a finite domain of length $l = 10$ with two absorbing boundaries. We compare the approximate parabolic solution of section 4.4 to SDE solutions of the Fokker–Planck equation, initialized either directly with the parabolic profile of equation (48) or with a point injection at $z_0 = 5$. The values for k and λ are determined from Equations (51) and

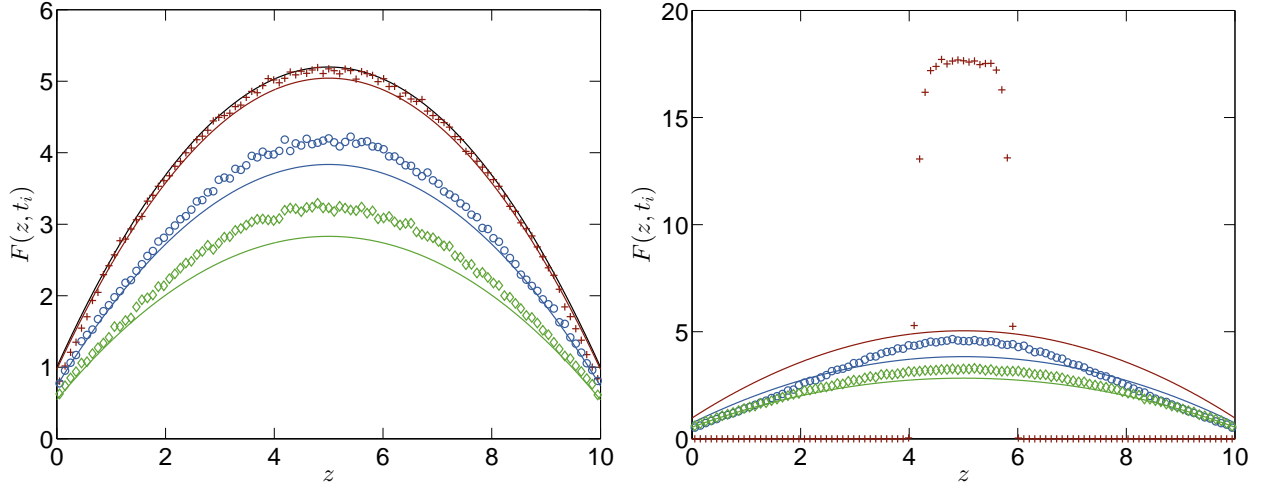


Fig. 5.— Comparison of the parabolic solution for the finite interval with absorbing boundaries (Equation (47), solid lines) to a SDE solution (symbols) of the Fokker–Planck equation with 10^6 particles initialized with the parabolic profile at $t = 0$ (solid black line) with a rejection sampling method (left panel) or with a point injection at $z_0 = 5$ (right panel). The three different times displayed are $t_1 = 1$ (red, '+'), $t_2 = 10$ (blue, 'o') and $t_3 = 20$ (green, '◇').

(53) as

$$\lambda = -0.0304 \quad (59)$$

$$k = 0.1679. \quad (60)$$

The second possible value for λ would result in a negative value for k giving an inverted parabolic profile.

Figure 5 shows the two cases (parabolic initial profile, left panel; delta-functional injection, right panel). For the left panel plot, the solutions have been normalized to agree for the initial profile. For the right panel, the solution is normalized to agree approximately at time $t_3 = 20$. It is clear that the parabolic solution captures both the general structure of the Fokker–Planck solution and its approximate exponential decay behavior quite well. The detailed time evolution and spatial dependence, however, are more complicated, and for the delta-functional injection, the parabolic profile only develops at a later stage. As mentioned before, in the context of the semi-infinite interval, the telegraph approximation allows for non-vanishing boundary values, in contrast to the boundary condition $F = F_0 = 0$ in the diffusion approximation. This appears to yield good agreement of the telegraph solution with the numerical Fokker–Planck results in the vicinity of the absorbing boundaries.

We could not confirm numerically the presence of discontinuities in the analytical solution of Masoliver et al. (1992) for the initial isotropic pitch-angle distribution of particles (see Dunkel et al. 2007, for discussion of this feature of the telegraph approximation, as well as for an alternative approach to diffusive transport modeling). An initial condition corresponding to two oppositely-traveling particle beams might give a better agreement of the numerical Fokker–Planck solution and the telegraph approximation.

6. Discussion

In this paper we systematically developed the telegraph approximation for particle transport in the presence of boundaries, taking into account the adiabatic focusing effect in a non-uniform mean magnetic field, which leads to coherent particle streaming along the field. We derived reflecting and absorbing boundary conditions for a modified telegraph equation with a convective term, and we presented analytical solutions of illustrative boundary problems, which might be relevant for modeling diffusive cosmic-ray transport in nonuniform large-scale magnetic fields in the presence of boundaries. We also demonstrated the accuracy of the telegraph approximation for focused transport in the presence of boundaries by comparing the analytical solutions of the telegraph approximation with the numerical solutions of the original Fokker–Planck equation. The numerical results complement those for an infinite interval (Litvinenko & Noble 2013; Effenberger & Litvinenko 2014).

The key point in assessing the practical usefulness of the telegraph model is that cosmic-ray transport in turbulent magnetic fields is diffusive on sufficiently long time scales. After a few scattering times, the diffusion and telegraph models give very similar predictions for an evolving particle distribution. The telegraph approximation is an attempt to more accurately describe the particle evolution on shorter time scales. Direct comparison of the predictions of the diffusion and telegraph models with the numerical solution of the Fokker–Planck equation for focused particle transport clearly shows that the telegraph model reproduces the shape of an evolving density pulse much better than the diffusion model, especially when focusing is strong, even for times significantly exceeding the scattering time (see, for instance, Figures 2 and 3 in Effenberger & Litvinenko 2014).

In the present study, we compared the Fokker–Planck and telegraph results for different boundary value problems and confirmed the validity of the telegraph approximation after just a few scattering times. Hence the telegraph approximation can provide an improved description over the diffusion approximation at these early times. Values for the parallel mean free path of about 0.1 to 0.3 AU, found in solar energetic particle studies (e.g. Dröge et al. 2014), suggest that the time scale of a few scattering times is relevant for interplanetary

particle transport, for example in the problem of predicting the impact of large solar events at 1 AU (e.g. Shea & Smart 2012).

A limitation of the telegraph approximation is that solving an initial value problem requires the knowledge of the first derivative of the density $F_0(z, t)$ with respect to time at $t = 0$, which can be determined only if the full distribution function $f_0(z, \mu, v, t)$ is known. However, in concrete applications $\partial_t F_0(z, 0)$ may be known or estimated either observationally or on theoretical grounds. For instance, in the simplest case of an isotropic initial distribution, the derivative vanishes (see equations 4 and 5 in Litvinenko and Schlickeiser 2014). More generally, any knowledge of the initial distribution would yield a more accurate description of the evolving particle distribution in the telegraph model, as compared with the diffusion model.

Finally, the telegraph equation proved to be a useful model in a wide range of transport problems (for a review, see Weiss 2002; Dunkel et al. 2007), and so the results of the present paper should have a broad applicability.

Y.L. thanks Prof. Reinhard Schlickeiser for supporting his visit to Ruhr-Universität Bochum, where a part of this work was completed. Travel support for F.E. from the International Space Science Institute for meetings of the international team 297 is appreciated. R.S. acknowledges support by the Deutsche Forschungsgemeinschaft (grant Schl 201/29-1).

- Artmann, S., Schlickeiser, R., Agueda, N., Krucker, S., & Lin, R. P. 2011, A&A 535, A92
- Beeck, J., & Wibberenz, G. 1986, ApJ, 311, 437
- Bieber, J. W., Evenson, P. A., & Matthaeus, W. H. 1987, Geophys. Res. Lett., 14, 864
- Brinkman, H. C. 1956, Physica, 22, 29
- Crank, J. 1984, Free and Moving Boundary Problems (Oxford: Clarendon Press)
- Davies, R. W. 1954, Phys. Rev., 93, 1169
- Dresing, N., Gómez-Herrero, R., Heber, B., Klassen, A., Malandraki, O., Dröge, W., & Kartavykh, Y. 2014, A&A 567, A27
- Dröge, W., Kartavykh, Y. Y., Klecker, B., & Kovaltsov, G. A. 2010, ApJ, 709, 912

- Dröge, W., Kartavykh, Y. Y., Dresing, N., Heber, B., & Klassen, A. 2014, JGR, 119, 6074
- Dunkel, J., Talkner, P., & Hänggi, P. 2007, Phys. Rev. D, 75, 043001
- Earl, J. A. 1974, ApJ, 193, 231
- Earl, J. A. 1976, ApJ, 205, 900
- Earl, J. A. 1981, ApJ, 251, 739
- Earl, J. A. 1992, ApJ, 395, 185
- Effenberger, F., & Litvinenko, Y. E. 2014, ApJ, 783:15
- Erdélyi, A., Magnus, W., Oberhettinger, F., & Tricomi, F. G. 1954, Tables of Integral Transforms (New York: McGraw-Hill)
- Fisk, L. A., & Axford, W. I. 1969, Sol. Phys., 7, 486
- Goldstein, S. 1951, Quart. J. Mech. Appl. Math., 4, 129
- Gombosi, T. I., Jokipii, J. R., Kota, J., Lorencz, K., & Williams, L. L. 1993, ApJ, 403, 377
- Hasselmann, K., & Wibberenz, G. 1970, ApJ, 162, 1049
- He, H.-Q., & Schlickeiser, R. 2014, ApJ, 792, 85
- Hemmer, P. C. 1961, Physica, 27, 79
- Hill, J. M., & Dewynne, J. N. 1987, Heat Conduction (Oxford: Blackwell Scientific)
- Jokipii, J. R. 1976, ApJ, 208, 900
- Kevorkian, J. 2000, Partial Differential Equations: Analytical Solution Techniques (Berlin: Springer)
- Kopp, A., Büsching, I., Strauss, R. D., & Potgieter, M. S. 2012, Comp. Phys. Comm., 183, 530
- Kunstmann, J. 1979, ApJ, 229, 812
- Laitinen, T., Dalla, S., & Marsh, M. S. 2013, ApJ, 773, L29

- Lario, D., Raouafi, N. E., Kwoon, R.-Y., Zhang, J., Gómez-Herrero, R., Dresing, N., & Riley, P. 2014, *ApJ*, 797, 8
- Le Roux, J. A., & Webb, G. M. 2009, *ApJ*, 693, 534
- Litvinenko, Y. E. 2012a, *ApJ*, 745, 62
- Litvinenko, Y. E. 2012b, *ApJ*, 752, 16
- Litvinenko, Y. E., & Noble, P. L. 2013, *ApJ*, 765, 31
- Litvinenko, Y. E., & Schlickeiser, R. 2011, *ApJ*, 732, L31
- Litvinenko, Y. E., & Schlickeiser, R. 2013, *A&A*, 554, A59
- Malkov, M., & Sagdeev, R. 2015, arXiv:1502.01799
- Marshak, R. E. 1947, *Phys. Rev.*, 71, 443
- Masoliver, J., Pòrra, J. M., & Weiss, G. H. 1992, *Phys. Rev. A*, 45, 2222
- Masoliver, J., Pòrra, J. M., & Weiss, G. H. 1993, *Phys. Rev. E*, 48, 939
- Pauls, H. L., & Burger, R. A. 1994, *ApJ*, 427, 927
- Qin, G., Wang, Y. Zhang, M., & Dalla, S. 2013, *ApJ*, 766, 74
- Roelof, E. C. 1969, in *Lectures in High-Energy Astrophysics*, ed. H. Ögelman & J. R. Wayland, 111
- Sack, R. A. 1956, *Physica*, 22, 917
- Sandroos, A., & Vainio, R. 2007, *A&A*, 455, 685
- Schlickeiser, R. 2009, *Mod. Phys. Lett. A*, 24, 1461
- Schlickeiser, R. 2011, *ApJ*, 732, 96
- Schlickeiser, R., Artmann, S., & Zöller, C. 2011, *Nuclear Phys. B*, 212-213, 181
- Schlickeiser, R., & Shalchi, A. 2008, *ApJ*, 686, 292
- Schwadron, N. A., & Gombosi, T. I. 1994, *J. Geophys. Res.*, 99, 19301
- Shalchi, A. 2011, *ApJ*, 728, 113
- Shea, M. A., & Smart, D. F. 2012, *Space Sci. Rev.*, 171:161

- Sofue, Y., Fujimoto, M., & Wielebinski, R. 1986, ARA&A, 24, 459
- Wang, Y., & Qin, G. 2015, ApJ, 799, 111
- Weinberg, A. M., & Wigner, E. P. 1958, The Physical Theory of Neutron Chain Reactors (Chicago: University of Chicago Press), Chap. 8
- Weiss, G. H. 2002, Physica A, 311, 381
- Zhang, M., Qin, G., & Rassoul, H. 2009, ApJ, 692, 109